The Journal of Fourier Analysis and Applications
Volume 2, Number 2, 1995

Biorthogonal Smooth Local Trigonometric Bases

Björn Jawerth and Wim Sweldens

ABSTRACT. In this paper we discuss smooth local trigonometric bases. We present two generalizations of the orthogonal basis of Malvar and Coifman-Meyer: biorthogonal and equal parity bases. These allow natural representations of constant and, sometimes, linear components. We study and compare their approximation properties and applicability in data compression. This is illustrated with numerical examples.

1. Introduction

Many applications in signal and image processing call for the use of basis functions that are local in time (or space) and frequency. The reason is that most signals have both temporal and spectral correlation and the use of basis functions that are local in time and frequency results in good approximation properties. Roughly speaking this means that we can obtain an approximation with a small error using only a few basis functions. This is the key to applications such as data compression.

One method of constructing such a basis is to use wavelets, which are translates and dilates of one particular function, the "mother wavelet." Another, rather trivial, way to construct an orthogonal basis with time-frequency localization is to divide the real axis into disjoint intervals and use Fourier series on each interval. We refer to such a basis as a *local trigonometric basis*. This basis, however, has several disadvantages.

1. Fourier series converge rapidly when the function is smooth and periodic. Evidently the restriction of a smooth function to an interval is in general not smooth and periodic. The convergence will thus be slow and the approximation properties poor.
2. Since each interval is handled separately, the approximations are, in general, discontinuous.
3. It is not immediately clear how to best divide the real axis into intervals.

An improvement was proposed by R. Coifman and Y. Meyer [7] and by H. Malvar [12, 13]. The idea is to use smooth cut-off functions to split the function and to "fold" overlapping parts in a clever way back into the intervals so that the orthogonality is preserved. Moreover, by choosing

Math Subject Classification. 42A10, 42A16.
Keywords and Phrases. Local trigonometric basis, wavelet, biorthogonality, data compression.
Acknowledgements and Notes. Björn Jawerth was partially supported by DARPA Grant AFOSR F49620-93-1-0083 and ONR Grant N00014-90-J-1343. Wim Sweldens was partially supported by NSF EPSCoR Grant EHR 9108772 and DARPA Grant AFOSR F49620-93-1-0083. He is also Senior Research Assistant of the National Fund of Scientific Research Belgium (NFWO).
All experiments were done and all graphs were made using Matlab.
After completing this work, we learned that similar results were obtained by G. Matviyenko. His approach is different in the sense that he tries to modify the shape of the bell function in order to get efficient compression of trigonometric functions. We refer to [14] for details.

ISSN 1069-5869

the right trigonometric basis, rapid convergence in the case of smooth functions is ensured. We refer to such a basis as a *smooth local trigonometric basis*. This approach essentially solves the first two disadvantages described above. An expository paper can be found in [4]. In [3], a connection between this basis and the Wilson basis of [9] was pointed out. Smooth local trigonometric bases were used successfully for image compression in [1, 2, 11].

The third disadvantage can be resolved by using an adaptive algorithm where the splitting locations are allowed to depend on the function. An algorithm was presented by R. Coifman and V. Wickerhauser in [8, 20]. An improvement was proposed in [10].

The basis of Coifman and Meyer has the disadvantage that the resolution of the constant is lost; i.e., on each interval the constant function is not a basis function. In this paper we present two generalizations that preserve the resolution of the constant. The first one is based on a construction of so-called biorthogonal folding operators, while the second employs *equal parity folding* (EPF). We also show how to adapt the construction for bounded domains.

This paper is organized as follows. In the first section we discuss trigonometric bases and their properties. In §4 we consider the basis of Coifman and Meyer. We present their construction from a different angle than in the original paper so as to facilitate the presentation of the biorthogonal construction in §6. We study the connection between smooth local trigonometric bases and wavelets in §5. In §7 we address the construction on an interval. Section 8 contains a discussion of equal parity folding. Finally, in §§9 and 10, we consider some implementation issues and give numerical results.

2. Notation and Terminology

Much of the notation will be presented as needed. The space of *square integrable functions*, $L^2(\mathbf{R})$ or L^2 for short, is defined as the space of Lebesgue measurable functions for which

$$\|f\|^2 = \int_{-\infty}^{+\infty} |f(x)|^2 \, dx < \infty.$$

The *inner product* of two functions $f, g \in L^2$ is given by

$$\langle f, g \rangle = \int_{-\infty}^{+\infty} f(x) \, \overline{g(x)} \, dx.$$

An operator is a linear map from L^2 to itself. The *norm* of an operator T is defined as

$$\|T\| = \sup_{\|f\|=1} \|T f\|.$$

The *adjoint* T^* of an operator T satisfies

$$\langle T f, g \rangle = \langle f, T^* g \rangle,$$

for all f and g in L^2. The *kernel* of an operator is given by

$$\ker T = \{x \in L^2 \mid T x = 0\},$$

and its *range* by

$$\text{range } T = \{Tx \mid x \in L^2\}.$$

An operator is *invertible* if its kernel is equal to {0} and if a bounded operator G exists so that $GF = FG = \mathbf{1}$. The *condition number* of an operator is defined as $\kappa = \|T\| \cdot \|T^{-1}\|$. An operator is *selfadjoint* in the case $T^* = T$ and *unitary* in the case $T^{-1} = T^*$.

A countable subset $\{f_n\}$ of L^2 is a *Riesz basis* if every element $f \in \mathrm{L}^2$ can be written uniquely as $f = \sum_n c_n f_n$ and if there are positive constants A and B such that

$$A \|f\|^2 \;\leq\; \sum_n |c_n|^2 \;\leq\; B \|f\|^2.$$

A Riesz basis is an *orthogonal basis* in the case the f_n are mutually orthogonal. In this case $A = B = 1$.

A bounded function f satisfies a *Lipschitz condition* of order λ ($0 < \lambda \leq 1$) on a set S if

$$|f(x) - f(y)| \;=\; \mathcal{O}(|x - y|)^{\lambda}) \qquad \text{for} \quad x, y \in S.$$

We then say it belongs to the space $\mathrm{Lip}^{\lambda}(S)$. Higher order Lipschitz regularity ($\lambda > 1$) can be defined in a straightforward way by using higher order differences of f.

The *Fourier transform* of a function $f \in \mathrm{L}^2$ is defined as

$$\widehat{f}(\omega) \;=\; \int_{-\infty}^{+\infty} f(x)\, e^{-i\omega x}\, dx.$$

3. Trigonometric Bases

Consider the interval $I = [0, 1]$ for simplicity. The basis functions of a Fourier series are given by

$$e_k(x) \;=\; \exp(i 2\pi k x),$$

and we know that the set $\{e_k\}$ is an orthonormal basis for $\mathrm{L}^2([0, 1])$. The Fourier series of a function is given by

$$f \;=\; \sum_k c_k\, e_k, \quad \text{with} \quad c_k \;=\; \int_0^1 f(x)\, \overline{e_k(x)}\, dx.$$

The decay of the coefficients, and thus the convergence rate, depends on the smoothness of f when I is identified with the torus τ (i.e. the smoothness of the periodic extension of f). More precisely, if $f \in \mathrm{Lip}^{\lambda}(\tau)$, then

$$c_k \;=\; \mathcal{O}(|k|^{-\lambda}); \tag{1}$$

see [21]. This property is fundamental. It tells us that if the function is smooth, the convergence will be rapid. By truncating the series we thus obtain accurate approximations.

However, as we already hinted in the introduction, the restriction to an interval of a smooth function defined on the real line is not necessarily a smooth function when extended periodically. Obviously, the behavior of a function on the left end of the interval does not necessarily match the behavior on the right end. The convergence can thus be slow and the approximation properties poor.

Other orthonormal bases that only have sines or cosines as basis functions exist. One of them is the sine IV basis where

$$s_k(x) \;=\; \sin\frac{2k+1}{2}\pi x,$$

and the set $\{\sqrt{2}\,s_k \mid k \in \mathbf{N}\}$ is an orthonormal basis for $\mathrm{L}^2([0,1])$. It is called the sine IV basis because it uses basis functions that have quarter wavelengths as compared to the Fourier series. The functions s_k are odd and smooth around the left endpoint and even and smooth around the right endpoint. Other basis functions and their parity are: sine II (odd and odd),

$$S_k(x) \;=\; \sin k\pi x;$$

cosine II (even and even),

$$C_k(x) \;=\; \cos k\pi x;$$

and cosine IV (even and odd),

$$c_k(x) \;=\; \cos\frac{2k+1}{2}\pi x.$$

For each basis a discrete transform and a fast (linear) algorithm, inspired by the *Fast Fourier Transform* (FFT), exist; see [16, 18, 20]. Whenever the data shows some special behavior such as periodicity or parity around an endpoint, it is important to pick the basis that reflects this property in order to obtain the rapid decay of the coefficients (cf. (1)).

4. Local Trigonometric Bases of Coifman and Meyer

4.1. The Folding Operator

The *mirror operator* $\mathcal{M}_\alpha$ around a point α is defined as

$$\mathcal{M}_\alpha\, f(x) \;=\; f(2\alpha - x).$$

It essentially flips the function around α. Note that it is selfadjoint and unitary. Consider an interval of length $2\epsilon_\alpha$ around α and a continuous left cut-off function l so that

$$l_\alpha(x) \;=\; \begin{cases} 1 & \text{if} \quad x < \alpha - \epsilon_\alpha, \\ 0 & \text{if} \quad x > \alpha + \epsilon_\alpha; \end{cases}$$

and let the right cut-off function be $r_\alpha = \mathcal{M}_\alpha\, l_\alpha$. Also let $\chi^l_\alpha = \chi_{(-\infty,\alpha]}$ and $\chi^r_\alpha = \chi_{[\alpha,\infty)}$. The following preposition lists some of the commutation properties of the mirror operator and cut-off functions.

1. ***Preposition***

The mirror operator and cut-off functions satisfy

$$\mathcal{M}_\alpha\, l_\alpha = r_\alpha\, \mathcal{M}_\alpha, \qquad \mathcal{M}_\alpha\, r_\alpha = l_\alpha\, \mathcal{M}_\alpha,$$
$$\mathcal{M}_\alpha\, \chi^l_\alpha = \chi^r_\alpha\, \mathcal{M}_\alpha, \qquad \mathcal{M}_\alpha\, \chi^r_\alpha = \chi^l_\alpha\, \mathcal{M}_\alpha.$$

Note that we use the same symbol for a function and for the operator defined as multiplication with that function. We now define the folding operator.

Definition 2. The *folding operator* around a point α is defined as

$$\mathcal{F}_\alpha \;=\; \chi_\alpha^l\,(1+\mathcal{M}_\alpha)\,l_\alpha + \chi_\alpha^r\,(1-\mathcal{M}_\alpha)\,r_\alpha. \qquad \square$$

Using simple algebraic manipulations and Preposition , it is easily checked that the adjoint of the folding operator is given by

$$\begin{aligned}\mathcal{F}_\alpha^* &= l_\alpha\,(1+\mathcal{M}_\alpha)\,\chi_\alpha^l + r_\alpha\,(1-\mathcal{M}_\alpha)\,\chi_\alpha^r \\ &= \chi_\alpha^l\,(1-\mathcal{M}_\alpha)\,l_\alpha + \chi_\alpha^r\,(1+\mathcal{M}_\alpha)\,r_\alpha.\end{aligned}$$

3. ***Lemma***
The folding operator is unitary if and only if $l_\alpha^2 + r_\alpha^2 \;=\; 1$.

Proof. This follows from the fact that

$$\begin{aligned}\mathcal{F}_\alpha^*\,\mathcal{F}_\alpha \;&=\; l_\alpha\,(1+\mathcal{M}_\alpha)\,\chi_\alpha^l\,(1+\mathcal{M}_\alpha)\,l_\alpha + r_\alpha\,(1-\mathcal{M}_\alpha)\,\chi_\alpha^r\,(1-\mathcal{M}_\alpha)\,r_\alpha \\ &=\; l_\alpha^2\,\chi_\alpha^l + l_\alpha^2\,\chi_\alpha^r + l_\alpha\,\chi_\alpha^r\,r_\alpha\mathcal{M}_\alpha + l_\alpha\,\chi_\alpha^l\,r_\alpha\mathcal{M}_\alpha \\ &\quad + r_\alpha^2\,\chi_\alpha^r + r_\alpha^2\,\chi_\alpha^l - l_\alpha\,\chi_\alpha^r\,r_\alpha\mathcal{M}_\alpha - l_\alpha\,\chi_\alpha^l\,r_\alpha\mathcal{M}_\alpha \\ &=\; l_\alpha^2 + r_\alpha^2 \;=\; \mathcal{F}_\alpha\,\mathcal{F}_\alpha^*. \qquad \square\end{aligned}$$

For the remainder of §4 we assume that this condition is satisfied.

Let us try to understand how the folding operator behaves. Multiplication with l_α lets a function die off smoothly to the left of $\alpha+\epsilon_\alpha$. The operator $1+\mathcal{M}_\alpha$ then adds this function to its mirrored version. This results in a function even around α. This function is now cut off by χ_α^l. The right part is similar and creates an odd function. Consequently, if f is smooth, then $\chi_\alpha^l\,\mathcal{F}_\alpha\,f$ is a function that is smooth when extended "even" to the right and $\chi_\alpha^r\,\mathcal{F}_\alpha\,f$ is a function that is smooth when extended "odd" to the left. By extending as an even (resp., odd) function we mean applying the operator $1+\mathcal{M}$ (resp., $1-\mathcal{M}$).

Note that even when f is smooth, $\mathcal{F}_\alpha\,f$, in general, is discontinuous at α. The adjoint operator (which is also the inverse) does exactly the same but switches even and odd. Figure 1 shows the folding of a function around $\alpha = 0$.

4.2. The Total Folding Operator

Consider a partition of the real line $\mathbf{R}$ into disjoint set of intervals $I = (\alpha, \beta]$, so that

$$\mathbf{R} \;=\; \bigcup_I I,$$

and

$$\beta - \alpha \;\geq\; \epsilon_\alpha + \epsilon_\beta.$$

The operators $\mathcal{F}_\alpha$ and $\mathcal{F}_\beta$ commute because $\mathcal{F}_\alpha \equiv 1$ on $\mathbf{R}\setminus(\alpha-\epsilon_\alpha, \alpha+\epsilon_\alpha)$. This allows us to give the following definition.

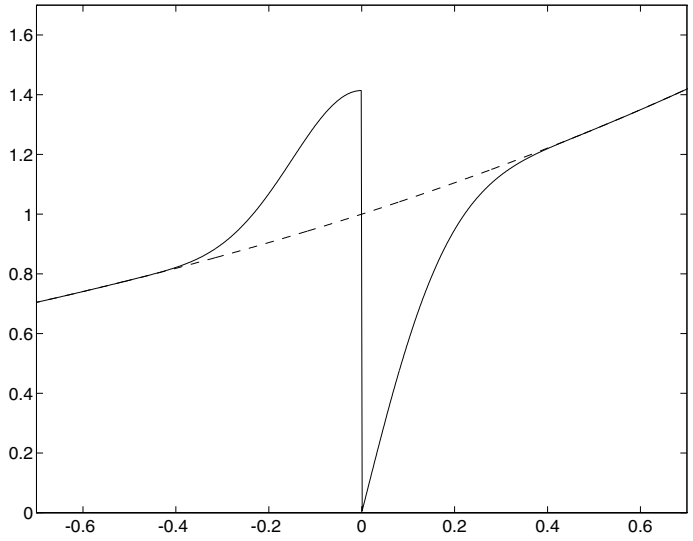

FIGURE 1. The folding of a function where $\alpha = 0$ and $\epsilon_\alpha = 0.5$.

Definition 4. The total folding operator is defined as

$$\mathcal{T} \;=\; \prod_{\alpha} \mathcal{F}_\alpha,$$

where the ordering in the product is arbitrary. □

Being a product of unitary operators, $\mathcal{T}$ too is unitary.

Next we rewrite the total folding operator as a sum of operators $\mathcal{G}_I$, each valid on the interval I, as

$$\mathcal{T} \;=\; \sum_{I} \chi_I \, \mathcal{G}_I.$$

One can understand that $\mathcal{G}_I$ is given by

$$\mathcal{G}_I \;=\; (1 - \mathcal{M}_\alpha + \mathcal{M}_\beta)\, b_I,$$

where b_I is the *bell function* associated with the interval I,

$$b_I \;=\; r_\alpha \, l_\beta.$$

This follows from the fact that in both representations of $\mathcal{T}$ we have

$$\mathcal{T} \;=\; \begin{cases} 1 & \text{on} \quad (\alpha + \epsilon_\alpha, \beta - \epsilon_\beta), \\ (1 - \mathcal{M}_\alpha)\, r_\alpha & \text{on} \quad (\alpha, \alpha + \epsilon_\alpha], \\ (1 + \mathcal{M}_\beta)\, l_\beta & \text{on} \quad [\beta - \epsilon_\beta, \beta]. \end{cases}$$

Note that

$$\mathcal{G}_I^* \;=\; b_I\,(1-\mathcal{M}_\alpha+\mathcal{M}_\beta)$$

and

$$\sum_I b_I^2 \;=\; 1.$$

We next study the properties of $\mathcal{G}_I$.

Definition 5. A function f is *locally even* (resp., *odd*) around a point α if $f(x)=\mathcal{M}_\alpha f(x)$ (resp., $-\mathcal{M}_\alpha f(x)$) for $x\in[\alpha-\epsilon_\alpha,\alpha+\epsilon_\alpha]$. □

6. ***Lemma***
The function $\mathcal{G}_I\ f$ is locally odd around α and locally even around β.

Proof. On the interval $[\alpha-\epsilon_\alpha,\alpha+\epsilon_\alpha]$, $\mathcal{G}_I\ f=(1-\mathcal{M}_\alpha)\,r_\alpha\ f$, so that $\mathcal{M}_\alpha\,\mathcal{G}_I\ f=-\mathcal{G}_I\ f$. On the interval $[\beta-\epsilon_\beta,\beta+\epsilon_\beta]$, $\mathcal{G}_I\ f=(1+\mathcal{M}_\beta)\,l_\beta\ f$, so that $\mathcal{M}_\beta\,\mathcal{G}_I\ f=\mathcal{G}_I\ f$. □

7. ***Lemma***
If a function s is locally odd around α and locally even around β, then

$$\chi_I\,\mathcal{G}_I\,b_I\,s \;=\; \chi_I\,s \quad\textit{and}\quad \mathcal{G}_I^*\,\chi_I\,s \;=\; b_I\,s.$$

Proof. We prove the first equation. On the interval $(\alpha+\epsilon_\alpha,\beta-\epsilon_\beta)$, the left- and right-hand sides are equal to s. On the interval $(\alpha,\alpha+\epsilon_\alpha]$, the left-hand side is equal to $(1-\mathcal{M}_\alpha)\,r_\alpha^2\,s$, which is equal to s because s is locally odd and $r_\alpha^2+l_\alpha^2=1$. The interval $[\beta-\epsilon_\beta,\beta]$ and the second equation may be handled similarly. □

4.3. Splitting Into Subspaces

Our basic goal is to split L^2 into subspaces so that each subspace contains functions localized around one of the intervals I. Moreover, we want a basis that is suited for representation of smooth functions on that interval. The easiest would be to let

$$\mathrm{L}^2(\mathbf{R}) \;=\; \bigoplus_I \mathrm{L}^2(I).$$

This obviously is an orthogonal decomposition and multiplication with χ_I is the orthogonal projection associated with it. Unfortunately, the trigonometric basis on each interval has, in general, poor approximation properties; cf. the discussion in §3. The total folding operator, however, transforms a smooth function into a function with specific parity properties at the endpoints of each interval. If we then use a trigonometric basis that reflects these parities, we again get good approximation properties. The orthogonality is preserved because the total folding operator is unitary. The orthogonal projection operator associated with an interval is given by

$$\mathcal{P}_I \;=\; \mathcal{T}^*\,\chi_I\,\mathcal{T}.$$

We decompose $\mathrm{L}^2(\mathbf{R})$ into orthogonal subspaces as

$$\mathrm{L}^2(\mathbf{R}) \;=\; \bigoplus_I V_I \quad\text{with}\quad V_I \;=\; \mathcal{P}_I\,\mathrm{L}^2(\mathbf{R}).$$

It is immediately clear that

$$\mathcal{T}\, V_I \;=\; \mathrm{L}^2(I) \quad \text{and} \quad \mathcal{T}^*\, \mathrm{L}^2(I) \;=\; V_I.$$

Using folding operators associated with an interval, we can also write the projection operator as

$$\mathcal{P}_I \;=\; \mathcal{G}_I^*\, \chi_I\, \mathcal{G}_I.$$

8. ***Lemma***

Each element of V_I is of the form $b_I\, s$, where s is locally odd around α and locally even around β, and every function of this form belongs to V_I.

Proof. The first part follows from Lemma 6 and the fact that

$$\mathcal{P}_I \;=\; b_I\, \mathcal{G}_I,$$

which, in turn, is a consequence of Lemma 6 and the second part of Lemma 7.

The second part follows from the fact that if s is locally odd around α and locally even around β, then

$$\mathcal{P}_I\, b_I\, s \;=\; \mathcal{G}_I^*\, \chi_I\, \mathcal{G}_I\, b_I\, s \;=\; b_I\, s,$$

which is a consequence of Lemma 7 (first and second parts). □

The fact that the projection operators are orthogonal can also be understood as follows. Let I and J be two intervals. In the case they are not neighbors, the supports of $\mathcal{P}_I f$ and $\mathcal{P}_J g$ do not intersect. In the case that I and J meet at a point α, $\mathcal{P}_I f\, \mathcal{P}_J g$ is only supported on $[\alpha - \epsilon_\alpha, \alpha + \epsilon_\alpha]$, where it is equal to $b_I\, s\, b_J\, t = l_\alpha\, r_\alpha\, s\, t$. Here s is locally odd and t is locally even around α. Since $l_\alpha\, r_\alpha$ is locally even, the integral vanishes.

The previous lemma tells us which trigonometric basis is the right one to use. The orthonormal basis for $\mathrm{L}^2(I)$ that matches the parity is given by

$$\chi_I\, s_{I,k},$$

where

$$s_{I,k} \;=\; \sqrt{\frac{2}{|I|}}\, \sin \frac{2k+1}{2}\, \frac{\pi}{|I|}\, (x - \alpha).$$

This immediately corresponds to an orthogonal basis for V_I given by

$$\mathcal{T}^*\, \chi_I\, s_{I,k} \;=\; \mathcal{G}_I^*\, \chi_I\, s_{I,k} \;=\; b_I\, s_{I,k}, \quad \text{with} \quad k \in \mathbf{N}.$$

Consequently,

$$f \;=\; \sum_I \mathcal{P}_I f \;=\; \sum_{I,k} c_{I,k}\, b_I\, s_{I,k},$$

where the coefficients are given by

$$c_{I,k} \;=\; \langle\, f, b_I\, s_{I,k} \,\rangle \;=\; \langle\, \mathcal{T} f, \chi_I\, s_{I,k} \,\rangle\,. \tag{2}$$

If we look at the operators from a practical point of view, we see that $\mathcal{F}_\alpha$ (and thus $\mathcal{T}$), χ_I, and their adjoints are easy to discretize and to implement. This means we always use the second expression of (2) for the coefficients of a function. In addition, the machinery for local trigonometric bases on an interval then becomes readily available.

We can summarize the results from this section in the following theorem.

9. *Theorem*

Using the notation of this section, and assuming that $l_\alpha^2 + r_\alpha^2 = 1$, *the functions* $\{b_I\, s_{I,k}\}$ *form an orthogonal basis for* L^2. *Moreover, if* f *and the cut-off functions belong to* $\mathrm{Lip}^\lambda[\alpha - \epsilon_\alpha, \beta + \epsilon_\beta]$ *with* $I = (\alpha, \beta]$, *the coefficients of* f *decay as*

$$c_{I,k} \;=\; \mathcal{O}(k^{-\lambda}).$$

Note that the decay of the coefficients associated with the interval I only depends on the smoothness of f in the neighborhood of I.

5. Connection with Wavelets

There is a close connection between local trigonometric bases and wavelets. To understand this, we take a look at the following example. Consider the multiresolution analysis formed by the Shannon wavelet. Let

$$\psi(x) \;=\; \frac{\sin(2\pi x) - \sin(\pi x)}{\pi x}$$

and

$$\psi_{j,l}(x) \;=\; 2^{j/2}\, \psi(2^j x - l).$$

Define

$$W_j \;=\; \text{clos span}\, \{\psi_{j,l} \mid l \in \mathbf{Z}\}.$$

Then

$$\bigoplus_j W_j \;=\; \mathrm{L}^2(\mathbf{R}),$$

and the $\{\psi_{j,l}\}$ form an orthogonal basis for L^2.

Since

$$\widehat{\psi}(\omega) \;=\; \chi_I(\omega) \quad \text{with} \quad I = [-2\pi, -\pi] \cup [\pi, 2\pi],$$

we see that

$$W_j \;=\; \{f \in \mathrm{L}^2 \mid \text{supp}\, \widehat{f} \subset 2^j\, I\}.$$

The splitting of L^2 into the wavelet spaces thus corresponds to splitting the frequency axis into logarithmic intervals and letting

$$\mathrm{L}^2 \;=\; \bigoplus \mathrm{L}^2(2^j\, I).$$

If we look at the Fourier transform of the wavelets,

$$\widehat{\psi}_{j,l} \;=\; \sqrt{2^{-j}} e^{-i\omega l 2^{-j}}\, \chi_{2^j I},$$

we see that they form a (nonsmooth) local trigonometric basis. These wavelets are not very useful in practice since they have slow decay. Remember that decay in the spatial domain corresponds to smoothness in the frequency domain. As we see, their Fourier transform has discontinuities.

It immediately follows that using the *smooth* local trigonometric basis on these intervals in the frequency domain leads to wavelets with rapid decay in the spatial domain. In case the cut-off functions belong to $\mathcal{C}^\infty$, the wavelets have faster than polynomial decay. The Meyer wavelet [15] was constructed in this way, and its generalization was one of the motivations for the work of Coifman and Meyer. These wavelets have an infinite number of vanishing moments since their Fourier transform vanishes in a neighborhood of the origin. Note that a splitting into intervals of equal size corresponds to a certain set of wavelet packets [10].

6. Biorthogonal Local Trigonometric Bases

An important property of a basis concerns how constant functions are represented. We say that a basis has a *resolution of the constant* if, on a finite domain, the constant is represented with a finite number of basis functions. Since a smooth function locally resembles a constant, it is important to represent a constant on each interval with as few coefficients as possible in order to get good approximation properties. For example, suppose we have an image with a constant background. Surely, we do not want to spend many coefficients in the representation of the background.

We adapt the construction so that the constant is one of the basis functions. From the previous section we see that

$$\chi_I \mathcal{G}_I 1 \;=\; \begin{cases} r_\alpha - l_\alpha & \text{on} \quad (\alpha, \alpha + \epsilon_\alpha], \\ 1 & \text{on} \quad (\alpha + \epsilon_\alpha, \beta - \epsilon_\beta), \\ r_\beta + l_\beta & \text{on} \quad [\beta - \epsilon_\beta, \beta]. \end{cases}$$

We want cut-off functions so that this function coincides with the first basis function $s_{I,0}$. This is clearly only possible if $\alpha + \epsilon_\alpha = \beta - \epsilon_\beta$. From now on, we therefore only work with intervals of equal size and let $\epsilon = |I|/2$. To achieve a resolution of the constant and still have an orthogonal basis, the cut-off function needs to be chosen as $l_\alpha = l((x - \alpha)/\epsilon)$, where

$$l(x) \;=\; \begin{cases} 1 & \text{for} \quad x < -1, \\ \dfrac{\cos(\pi x/4) - \sin(\pi x/4)}{\sqrt{2}} & \text{for} \quad x \in [-1, 1], \\ 0 & \text{for} \quad 1 < x. \end{cases}$$

This cut-off function is continuous but not differentiable. Consequently, the folding operator introduces discontinuities in derivatives that ruin the approximation properties (i.e., ruin the decay given in (1)). What we need is a resolution of the constant with smoother cut-off functions.

To solve this problem, we add some flexibility to the construction, by abandoning the orthogonality requirement. In the remainder of this paper we let l_α and $r_\alpha = \mathcal{M}_\alpha l_\alpha$ be continuous cut-off functions that do not necessarily satisfy $l_\alpha^2 + r_\alpha^2 = 1$.

10. ***Lemma***

In the case $l_\alpha^2 + r_\alpha^2$ is bounded from below and above, the folding operator is bounded and invertible. More precisely,

$$A \, \|f\| \;\leq\; \|\mathcal{F}_\alpha f\| \;\leq\; B \, \|f\|,$$

where

$$A \;=\; \min_x \sqrt{l_\alpha^2 + r_\alpha^2} \quad \textit{and} \quad B \;=\; \max_x \sqrt{l_\alpha^2 + r_\alpha^2},$$

and these constants are sharp.

Proof. The lemma follows from the fact that

$$\int_{-\infty}^{+\infty} |\mathcal{F}_\alpha f|^2 \, dx \;=\; \int_{-\infty}^{+\infty} (l_\alpha^2 + r_\alpha^2) \, |f|^2 \, dx,$$

which is the result from simple algebraic manipulations similar to those in the previous section. □

11. ***Lemma***

The inverse of an invertible folding operator $\mathcal{F}_\alpha$ is again a folding operator.

Proof. The equation $g = \mathcal{F}_\alpha f$ can be written in matrix form as

$$\chi_\alpha^l \begin{bmatrix} g \\ \mathcal{M}_\alpha \, g \end{bmatrix} = \begin{bmatrix} l_\alpha & r_\alpha \\ -r_\alpha & l_\alpha \end{bmatrix} \chi_\alpha^l \begin{bmatrix} f \\ \mathcal{M}_\alpha \, f \end{bmatrix}.$$

From this we see immediately that the inverse of $\mathcal{F}_\alpha$ is given by $\widetilde{\mathcal{F}_\alpha}^*$, where

$$\widetilde{\mathcal{F}_\alpha} \;=\; \chi_\alpha^l \, (1 + \mathcal{M}_\alpha) \, \tilde{l}_\alpha + \chi_\alpha^r \, (1 - \mathcal{M}_\alpha) \, \tilde{r}_\alpha,$$

$$\tilde{l}_\alpha \;=\; \frac{l_\alpha}{l_\alpha^2 + r_\alpha^2}, \quad \text{and} \quad \tilde{r}_\alpha \;=\; \frac{r_\alpha}{l_\alpha^2 + r_\alpha^2}. \qquad \square$$

Note that

$$l_\alpha \, \tilde{l}_\alpha + r_\alpha \, \tilde{r}_\alpha \;=\; 1.$$

We call $\mathcal{F}_\alpha$ and $\widetilde{\mathcal{F}_\alpha}$ *biorthogonal folding operators* and refer to $\widetilde{\mathcal{F}_\alpha}$ more specifically as the *dual folding operator*.

This does not solve the problem completely. Indeed, if the cut-off functions belong to $\mathcal{C}^1$, the folded constant has derivative zero at $\alpha + \epsilon$ and thus never coincides with the first basis function $s_{I,0}$. We therefore generalize the construction further by allowing different parities. We want to have a folding operator that takes a smooth function into a function that is either odd at the left *and* right endpoints of an interval or even at both endpoints. One way to do so would be to use folding

operators with the same parity left and right of the folding point. Unfortunately, we show in the next lemma that these operators are not invertible.

12. ***Lemma***
A folding operator with the same parity left and right of the folding point is not invertible.

Proof. Consider the even–even case, and let

$$\mathcal{F}_\alpha \;=\; \chi_\alpha^l\,(1+\mathcal{M}_\alpha)\,l_\alpha + \chi_\alpha^r\,(1+\mathcal{M}_\alpha)\,r_\alpha.$$

The matrix representation leads to a matrix with determinant $l_\alpha^2 - r_\alpha^2$, which vanishes at the folding point. □

This basically tells us that the only way to get the same parity at both endpoints of an interval is to alternate the parity of folding operators. In other words, we need to change the parity from ... (odd–even) (odd–even) (odd–even) ... to ... (even–even) (odd–odd) (even–even) (odd–odd) .... This implies defining the total folding operator by alternating $\mathcal{F}_\alpha$ and $\mathcal{F}_\alpha^*$. In the intervals with (even–even) parity we use the cosine II basis, and in the intervals with (odd–odd) parity the sine II basis. To write this in more detail we let

$$\alpha_l \;=\; l\,|I|,$$

and to simplify notation, we replace every subscript α_l, or I, by the integer subscript l. The total folding operator is now given by

$$\mathcal{T} \;=\; \prod_l \mathcal{F}_{2l}\;\mathcal{F}_{2l+1}^*,$$

where the factors commute. Again this operator is invertible, and since the individual folding operators do not interact spatially, it also satisfies

$$A\,\|f\| \;\le\; \|\mathcal{T} f\| \;\le\; B\,\|f\|,$$

with the same constants as above. The dual total folding operator is defined similarly (just add the tildes) and again $\mathcal{T}^{-1} = \widetilde{\mathcal{T}}^*$. The condition number of the total folding operator is B/A.

Following a reasoning similar to the orthogonal case, we see that the total folding operator can also be written as a sum of folding operators associated with an interval,

$$\mathcal{T} \;=\; \sum_l \chi_l\,\mathcal{G}_l :$$

where

$$\mathcal{G}_{2l} \;=\; (1-\mathcal{M}_\alpha-\mathcal{M}_\beta)\,b_{2l}$$

and

$$\mathcal{G}_{2l+1} \;=\; (1+\mathcal{M}_\alpha+\mathcal{M}_\beta)\,b_{2l+1}.$$

The projection operator associated with an interval is given by

$$\mathcal{P}_l \;=\; \widetilde{\mathcal{T}}^*\,\chi_l\,\mathcal{T}.$$

We decompose $\mathrm{L}^2(\mathbf{R})$ into subspaces,

$$\mathrm{L}^2(\mathbf{R}) \;=\; \bigoplus_l V_l \quad \text{with} \quad V_l \;=\; \mathcal{P}_l\,\mathrm{L}^2(\mathbf{R}),$$

where

$$\mathcal{T}\,V_l \;=\; \mathrm{L}^2(I) \quad \text{and} \quad \widetilde{\mathcal{T}}^*\,\mathrm{L}^2(I) \;=\; V_l.$$

Again the projection operator can also be written as

$$\mathcal{P}_l \;=\; \widetilde{\mathcal{G}}_l^*\,\chi_l\,\mathcal{G}_l \;=\; \tilde{b}_l\,\mathcal{G}_l.$$

If l is odd (resp., even), an element of V_l can be written as $\tilde{b}_l$ times a function that is locally even (resp. odd) around α and β.

We use the basis functions with the right parity on each interval:

$$t_{2l,k} \;=\; \sqrt{\frac{2}{|I|}}\,\sin(k+1)\frac{\pi}{|I|}(x-2l), \qquad k \geq 0;$$

$$t_{2l+1,k} \;=\; \sqrt{\frac{2}{|I|}}\,\cos k\frac{\pi}{|I|}(x-2l-1), \qquad k \geq 1;$$

and

$$t_{2l+1,0} \;=\; \frac{1}{\sqrt{|I|}}.$$

Obviously, the $t_{l,k}$ with $l \in \mathbf{Z}$ and $k \in \mathbf{N}$ form an orthonormal basis for L^2. This implies that the basis formed by the $\widetilde{\mathcal{T}}^*\,\chi_l\,t_{l,k}$ is a Riesz basis for L^2. These functions are given by

$$\widetilde{\mathcal{T}}^*\,\chi_l\,t_{l,k} \;=\; \widetilde{\mathcal{G}}_l^*\,\chi_l\,t_{l,k} \;=\; \tilde{b}_l\,t_{l,k}.$$

Consequently,

$$f \;=\; \sum_l \mathcal{P}_l f \;=\; \sum_{l,k} c_{l,k}\,\tilde{b}_l\,t_{l,k},$$

where the coefficients are given by

$$c_{l,k} \;=\; \langle\,\mathcal{T} f, \chi_l\,t_{l,k}\,\rangle \;=\; \langle\,f, \mathcal{T}^*\,\chi_l\,t_{l,k}\,\rangle \;=\; \langle\,f, b_l\,t_{l,k}\,\rangle\,, \tag{3}$$

and

$$A\,\|f\| \;\leq\; \sqrt{\sum_{l,k} c_{l,k}^2} \;\leq\; B\,\|f\|,$$

with the same constants as above. We say that $\{b_l\, t_{l,k}\}$ is the dual basis corresponding to the basis $\{\tilde{b}_l\, t_{l,k}\}$. The first expression of (3) for the coefficients is the easiest to implement. We summarize the results in a theorem.

13. *Theorem*

With the notation of this section, the sets of functions $\{b_l\, t_{l,k}\}$ *and* $\{\tilde{b}_l\, t_{l,k}\}$ *are dual Riesz bases of* L^2. *More precisely, they are biorthogonal in the sense that*

$$\langle\, b_l\, t_{l,k}, \tilde{b}_{l'}\, t_{l',k'}\,\rangle \;=\; \delta_{l-l'}\,\delta_{k-k'}.$$

If f *and the cut-off functions belong to* $\mathrm{Lip}^{\lambda}[\alpha-\epsilon_\alpha, \beta+\epsilon_\beta]$ *with* $I=(\alpha,\beta]$, *the coefficients of* f *decay as*

$$c_{I,k} \;=\; \mathcal{O}(k^{-\lambda}).$$

Note that these bases still have some orthogonality. More precisely, two basis functions associated with different intervals are still orthogonal. This can be understood using a reasoning similar to that following Lemma 8. The splitting of L^2 into subspaces thus still is an orthogonal splitting.

The only thing left is to find cut-off functions so that $\chi_l\, \mathcal{T}\, 1$ coincides (up to a constant factor) with $\chi_l\, t_{l,0}$. This can be done by letting $l_\alpha = l((x-\alpha)/\epsilon_\alpha)$ where

$$l(x) \;=\; \frac{1-\sin(\pi x/2)}{2} \quad \text{for} \quad x\in[-1,1].$$

This cut-off function belongs to $\mathcal{C}^1$.

It is easy to check that on I,

$$\mathcal{G}_{2l}\, 1 \;=\; \sin\left(\frac{x-2l}{|I|}\right) \quad \text{and} \quad \mathcal{G}_{2l+1}\, 1 \;=\; 1.$$

In this case the constants A and B, used in the comparison of norms, are $1/\sqrt{2}$ and 1, respectively. The condition number of the folding operator is thus $\sqrt{2}$. We have chosen this normalization because it is natural for the cut-off functions to have the value $\frac{1}{2}$ at α. This means that the even side of the folded function coincides with the original function at the folding point. The cut-off functions are shown in Figure 2 and the biorthogonal total folding of an exponential function is shown in Figure 3. The folded function on each interval closely resembles the first basis function. Figure 4 shows two basis functions, $\widetilde{b}_2\, t_{2,4}$ and $\widetilde{b}_5\, t_{5,9}$, where $|I|=1$. The shape of the bell function is dotted. Note the parity of the basis functions at the endpoints.

7. Folding Operators on an Interval

So far we have only discussed functions defined on the real line. In this section, we focus on folding operators on an interval. Since we can treat each boundary point independently, we consider the case of the interval $I=[\alpha,\infty)$. We introduce an extension operator $\mathcal{S}$ that takes a function from $\mathrm{L}^2(I)$ to a function of $\mathrm{L}^2(\mathbf{R})$ and a restriction operator $\mathcal{R}=\chi_I$ that does the opposite. We want them to satisfy $\mathcal{R}\,\mathcal{S}=\mathbf{1}$ on $\mathrm{L}^2(I)$. Also, in the case f is smooth, we want $\mathcal{S}\,f$ to have some smoothness too. For notational simplicity, we omit the subscript α and introduce a superscript b for

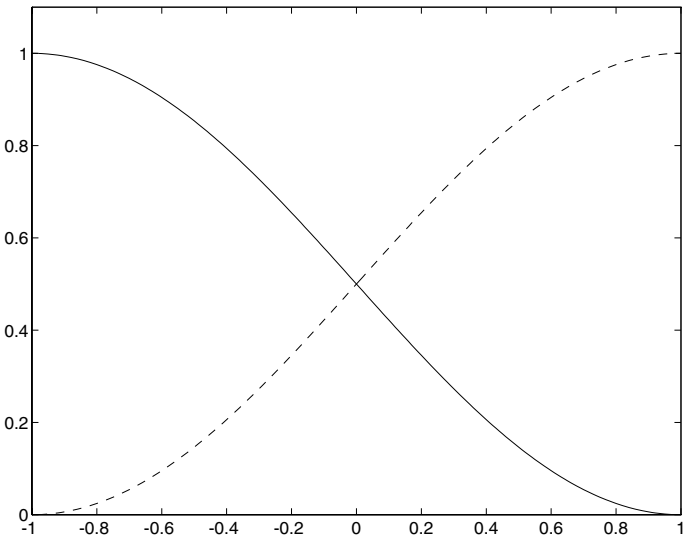

FIGURE 2. The biorthogonal cutoff functions.

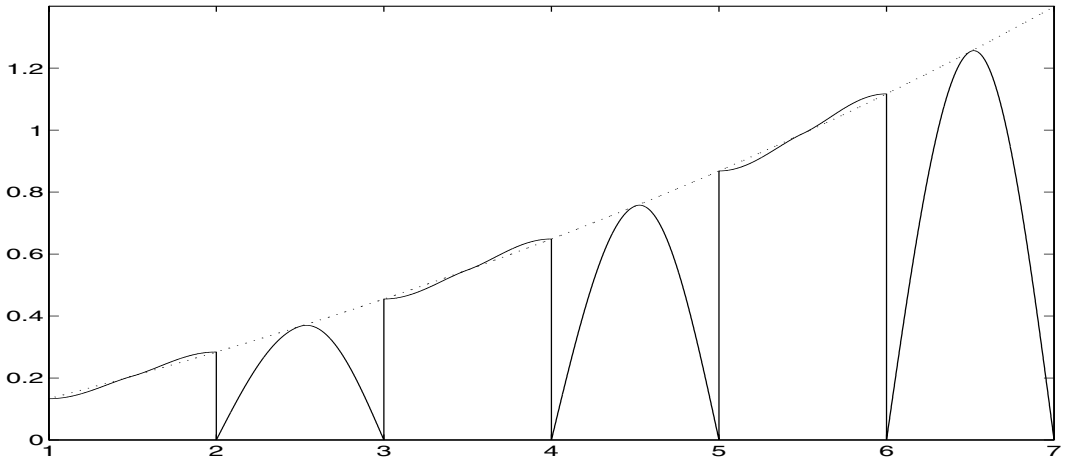

FIGURE 3. The biorthogonal folding.

cut-off functions and operators associated with the boundary of the interval. We define the folding operator at the boundary as $\mathcal{F}^b = \mathcal{R}\,\mathcal{F}\,\mathcal{S}$. Let $l^b = \mathcal{R}\,l$ (similarly for r), and let $\mathcal{M}^b$ be the operator that maps a function of $\mathrm{L}^2(I)$ to its mirror in $\mathrm{L}^2(\mathbf{R} \setminus I)$. Now,

$$\begin{aligned}\mathcal{F}^b\, f &= \mathcal{R}\,[\chi_l\,(1+\mathcal{M})\,l + \chi_r\,(1-\mathcal{M})\,r]\,\mathcal{S} \\ &= \mathcal{R}\,(1-\mathcal{M})\,r\,\mathcal{S} = r^b\, f - l^b\,\mathcal{R}\,\mathcal{M}\,\mathcal{S}\, f.\end{aligned}$$

The second term has a plus sign in the case of $\mathcal{F}^{*b} = \mathcal{R}\,\mathcal{F}^*\,\mathcal{S}$ (i.e., the even case).

Assuming that f is continuous, we choose the extension operator in the odd case as

$$\mathcal{S}\, f \;=\; 2f(\alpha) - \mathcal{M}^b\, f \quad \text{on} \quad \mathbf{R} \setminus I.$$

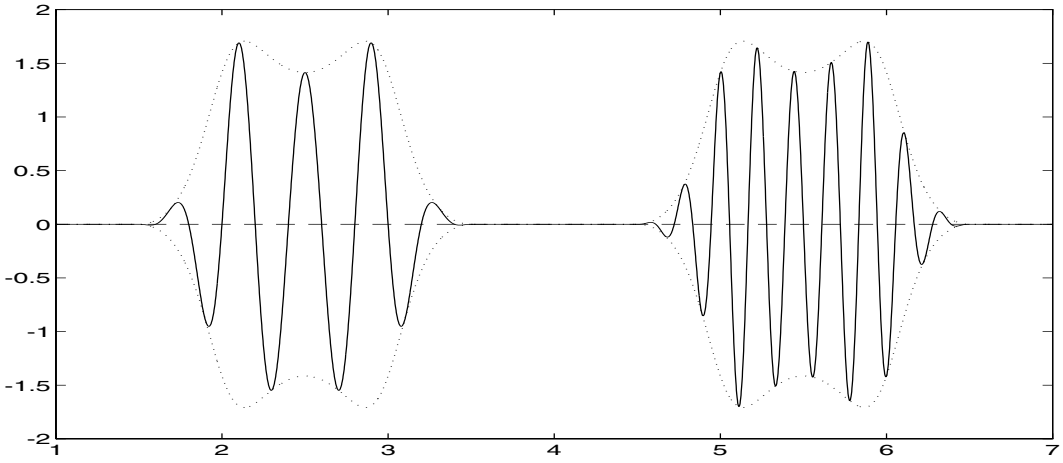

FIGURE 4. Biorthogonal basis functions.

This guarantees that if $f \in \mathcal{C}^1$, so is $\mathcal{S}\, f$. The folding operator is then given by

$$\mathcal{F}^b\, f \;=\; (l^b + r^b)\, f - 2 f(\alpha)\, l^b.$$

We can thus retrieve f from $\mathcal{F}^b\, f$ by

$$f \;=\; \frac{\mathcal{F}^b\, f + 2 f(\alpha)\, l^b}{l^b + r^b}.$$

This shows that we need $\mathcal{F}^b\, f$ *and* the value $f(\alpha)$ to find f again, which is no surprise because the folding operator can never "grasp" the value of f at α since $\mathcal{F}^b f(\alpha) = 0$ in the case f is continuous. We thus need to "store" separately the value $f(\alpha)$. The reconstruction step is stable since the denominator does not vanish.

If we use the same extension operator in the even case, the reconstruction becomes unstable since it has $l^b - r^b$ in the denominator. We therefore introduce the following extension operator in the even case:

$$\mathcal{S}\, f \;=\; \mathcal{M}^b\, f + 2 f'(\alpha)\, (x - \alpha) \quad \text{on} \quad \mathbf{R} \setminus I,$$

where we assume that $f \in \mathcal{C}^1$. Then $\mathcal{S} f \in \mathcal{C}^1$ as well. The folding operator is given by

$$\mathcal{F}^{*b} \;=\; (l^b + r^b)\, f + 2 f'(\alpha)\, (x - \alpha)\, l^b,$$

from which we see that the inverse operator again is stable. Here we need to "store" the value $f'(\alpha)$ separately.

The construction on the right boundary of an interval is analogous. Also, it is possible to construct extension operators that preserve more smoothness at a cost of having to store more information separately.

8. Equal Parity Folding

In this section we take a closer look at the folding operator that takes a smooth function into a function with the same parity left and right of the folding point. We call such a folding operator an

equal parity folding (EPF) operator. In §6 we proved that they are not invertible in L^2; see Lemma 12. Nevertheless, they have been used successfully for image compression; see [1]. In this section, we study their behavior more carefully and try to understand why they sometimes are useful.

We start by introducing two new operators $\mathcal{E}$ and $\mathcal{D}$ by

$$\mathcal{E} \;=\; 1 + \mathcal{M} \quad \text{and} \quad \mathcal{D} \;=\; 1 - \mathcal{M},$$

which map any function into an even (resp., odd) function and satisfy

$$\frac{\mathcal{E} + \mathcal{D}}{2} \;=\; 1.$$

Note that they are both selfadjoint and provide an orthogonal splitting of L^2 into $\mathcal{E}\,L^2 \oplus \mathcal{D}\,L^2$. We again take $\alpha = 0$ and omit the subscript α. We assume the cut-off functions to be continuous and satisfy

$$\lim_{x \to -\infty} l(x) \;=\; 1, \qquad \lim_{x \to +\infty} l(x) \;=\; 0, \tag{4}$$

and $r = \mathcal{M}\,l$. The EPF operator with (even–even) parity can now be written as

$$\mathcal{F} \;=\; \chi_l\,\mathcal{E}\,l + \chi_r\,\mathcal{E}\,r. \tag{5}$$

We immediately see that the EPF operator is selfadjoint. Also, it commutes with $\mathcal{M}$ and maps even (resp., odd) functions into even (resp., odd) functions. Next we study how the EPF operator behaves on the subspaces of even or odd functions.

14. ***Lemma***
On $\mathcal{E}\,L^2$, $\mathcal{F}$ coincides with $l + r$. On $\mathcal{D}\,L^2$, $\mathcal{F}$ coincides with $(\chi_l - \chi_r)\,(l - r)$.

Proof. If $f \in \mathcal{E}\,L^2$, we see that

$$\mathcal{F}\,f \;=\; \chi_l\,\mathcal{E}\,l\,f + \chi_r\,\mathcal{E}\,r\,\mathcal{M}\,f \;=\; \chi_l\,\mathcal{E}\,l\,f + \chi_r\,\mathcal{E}\,\mathcal{M}\,l\,f \;=\; \mathcal{E}\,l\,f.$$

If $f \in \mathcal{D}\,L^2$, we have

$$\mathcal{F}\,f \;=\; \chi_l\,\mathcal{E}\,l\,f - \chi_r\,\mathcal{E}\,r\,\mathcal{M}\,f \;=\; \chi_l\,\mathcal{E}\,l\,f - \chi_r\,\mathcal{E}\,l\,f \;=\; (\chi_l - \chi_r)\,(l - r)\,f. \qquad \square$$

We introduce two new functions e and d by

$$e \;=\; \mathcal{E}\,l \quad \text{and} \quad d \;=\; \mathcal{D}\,l.$$

The lemma implies that we can write $\mathcal{F}$ as

$$\mathcal{F} \;=\; e\,\mathcal{E} + d\,(\chi_l - \chi_r)\,\mathcal{D}. \tag{6}$$

This helps us to formulate the following lemmas.

15. ***Lemma***
The EPF operator is bounded.

Proof. This follows immediately from the representation (6), the fact that the cut-off functions are continuous, and their limit conditions (4). □

16. ***Lemma***
ker $f = \{0\}$.

Proof. From (5) we see that $\mathcal{F} f = 0$ implies that both lf and rf are odd. Consequently, ef and $d f$ are odd. The former implies that f is odd, the latter that f is even. Thus $f = 0$. □

We know that the kernel and the closure of the range of a selfadjoint operator form an orthogonal splitting of L^2. The former two lemmas thus imply that the range of $\mathcal{F}$ is dense in L^2. We show later that the range of $\mathcal{F}$ is actually a true subset of L^2.

17. ***Lemma***
The EPF operator is not invertible on its range.

Proof. Remember that an operator is invertible when its inverse exists and when the inverse is bounded. We prove that $\mathcal{F}$ is not invertible by constructing an odd function w with norm 1 so that $\mathcal{F} w$ can have arbitrarily small norm. Let

$$w = \frac{1}{2\sqrt{\delta}}\Big(\chi_{[-\delta,0]} - \chi_{[0,\delta]}\Big).$$

Then

$$\|\mathcal{F} w\| = \|d\, w\| \le \max_{x\in[-\delta,\delta]} d.$$

Since the cut-off functions are continuous, this can be made arbitrarily small. □

It is easy to see what the inverse operator, at least formally, looks like. It again is an EPF operator with the parity (even–even). We denote it by $\widetilde{\mathcal{F}}$ where

$$\widetilde{\mathcal{F}} = \tilde{e}\,\mathcal{E} + \tilde{d}\,(\chi_l - \chi_r)\,\mathcal{D},$$

with

$$\tilde{e} = \frac{1}{e} \quad \text{and} \quad \tilde{d} = \frac{1}{d}.$$

It immediately follows that formally $\widetilde{\mathcal{F}}\,\mathcal{F} = 1$. The inverse operator can also be written in a form similar to (5), where

$$\widetilde{\mathcal{F}} = \chi_l\,\mathcal{E}\,\tilde{l} + \chi_r\,\mathcal{E}\,\tilde{r},$$

with

$$\tilde{l} = \frac{l}{l^2 - r^2} \quad \text{and} \quad \tilde{r} = \frac{r}{r^2 - l^2}.$$

The fact that $\mathcal{F}$ is not invertible shows up here in the fact that $\tilde{d}$ has a singularity at $x = 0$. This also tells us that $\widetilde{\mathcal{F}}$ can take a function out of L^2, since this singularity is not necessarily square integrable.

We observe that $\mathcal{F}$ is bounded and invertible on the subspace of even functions in the case e is bounded away from 0 and ∞. For the odd functions we cannot make a similar statement as d always vanishes in the origin.

We can characterize the range of $\mathcal{F}$ by

$$\text{range } \mathcal{F} \;=\; \{f \in \mathrm{L}^2 \mid f/d \in \mathrm{L}^2\}.$$

If we also assume that the cut-off functions belong to $\mathcal{C}^1$, we see that $\tilde{d} = \mathcal{O}(1/x)$. This means that a function belongs to the range of $\mathcal{F}$ in the case it behaves like $\mathcal{O}(x^{1/2-\delta})$ in a neighborhood of the origin. A typical function that does not belong to the range of $\mathcal{F}$ is a function with a discontinuity at the folding point. Similarly we can describe the range of $\widetilde{\mathcal{F}}$ by

$$\text{range } \widetilde{\mathcal{F}} \;=\; \{f \in \mathrm{L}^2 \mid d\, f \in \mathrm{L}^2\},$$

and we note that $\mathrm{L}^2 \subset \text{range } \widetilde{\mathcal{F}}$. Again, a function that $\widetilde{\mathcal{F}}$ typically takes out of L^2 is a function with a discontinuity across the folding point. Under the assumption that the cut-off functions belong to $\mathcal{C}^1$, a function of the range of $\widetilde{\mathcal{F}}$ behaves like $\mathcal{O}(x^{-3/2-\delta})$ in a neighborhood of the origin.

We also note that $\mathcal{F}$ has some smoothing properties, i.e., it maps a function with a discontinuity at the origin into a continuous function since

$$\mathcal{F}\, \chi_l \;=\; l.$$

However, it does not smooth out discontinuities in the derivative because

$$\mathcal{F}\, x\, \chi_l \;=\; |x|\, l.$$

Let us discuss how these operators can be used for function approximation. The idea is to construct a total folding operator and then use a trigonometric basis with the right parity on each interval. In this case the right basis is the cosine II basis. We can find a nonlinear approximation by setting a fixed number of small coefficients to zero and applying the inverse total folding operator. If we think of $\mathcal{F}$ as a kind of smoothing operator and of $\widetilde{\mathcal{F}}$ as an operator that can blow up discontinuous functions, it makes sense to use $\widetilde{\mathcal{F}}$ to construct the total folding operator and $\mathcal{F}$ for its inverse. This has the following advantages.

- Since $\mathcal{F}$ is bounded, the error introduced by the approximation in the trigonometric basis cannot get magnified.
- Discontinuities across the folding points get smoothed by $\mathcal{F}$. In other words, the approximation has some smoothness.

We note that the idea to switch the two operators around was first suggested in [1].

This approach works well as long as the function is smooth at the folding point. This can be understood as follows. If a function is smooth, we can write a local first-order approximation as

$$f(x) \;\approx\; f(0) + f'(0)\, x + \mathcal{O}(x^2).$$

The first term is even and thus does not pose a problem as the folding operators are bounded and invertible on the space of even functions. The second term is odd but (locally) belongs to the range of $\mathcal{F}$ and thus does not cause any trouble. Problems, however, occur when the function is discontinuous at a folding point. We illustrate this with an example in the next section.

The construction of the total folding operators is analogous to the biorthogonal case, and we adopt the same notation (i.e., the integer subscripts). Evidently, there is no need to alternate the parities. On each interval we use the cosine II basis or the functions $\chi_l\, C_{l,k}$ where

$$C_{l,k} \;=\; \sqrt{\frac{2}{|I|}} \cos k \frac{\pi}{|I|}(x - 2l - 1).$$

It should be clear from the discussion above that the $\mathcal{F}\, \chi_l\, C_{l,k}$ cannot generate a basis for L^2 but merely form a set whose linear span is dense. We remark that we still have

$$\mathcal{F}\, \chi_l\, C_{k,l} \;=\; b_l\, C_{k,l},$$

where b_l is the usual bell function. So formally we can use this transform, but there is no guarantee that the coefficients will be bounded.

It is easy to see that we get a resolution of the constant in the case $e = 1$. But, unlike in the biorthogonal case, one degree of freedom is left after fixing the resolution of the constant, namely, the choice of d. We can use this to also obtain a *resolution of the linear*, i.e., a representation of each linear function by two basis functions on an interval. To do so we need to choose d so that

$$d(\epsilon\, x) \;=\; \frac{x}{1 - 2/\pi \cos(\pi x/2)} \quad \text{for} \quad x \in [-1, 1],$$

and, consequently,

$$l \;=\; \frac{1+d}{2} \quad \text{and} \quad r \;=\; \frac{1-d}{2}.$$

The function d is smooth and satisfies the right boundary conditions. Then, with $\epsilon = 1$,

$$\begin{aligned} \tilde{\mathcal{F}}\, x \;&=\; \tilde{e}\, \mathcal{E}\, x + \tilde{d}\, (\chi_l - \chi_r)\, \mathcal{D}\, x \\ &= \tilde{d}\, x \;=\; 1 - \frac{2}{\pi} \cos\left(\frac{\pi x}{2}\right). \end{aligned}$$

Figure 5 shows the l, r, and d functions in this case. Figure 6 shows the equal parity folding of the function x with folding points 0 and 1 and $\epsilon = 0.5$. We see that on the interval [0,1] it coincides with a function of the form $A + B \cos(\pi x)$ (dashed).

9. Implementation and Results

So far the discussion has only concerned functions of a continuous variable. In applications the construction needs to be discretized. A function f is then given as a sequence $\{f_n\}$ where the "samples" f_n can be seen as pointwise evaluations on a regular grid in the case f is continuous or as average values of f in a neighborhood of the grid point if not. For each local trigonometric basis, a discrete implementation of the transform is available, which is based on the FFT. The implementation of the FFT is most straightforward in case the number of samples is a power of two.

We first need to decide whether we want to use a staggered or nonstaggered discretization. In a *nonstaggered discretization*, the boundaries of the interval coincide with a grid point, while in a *staggered discretization*, the boundaries of the interval fall between grid points.

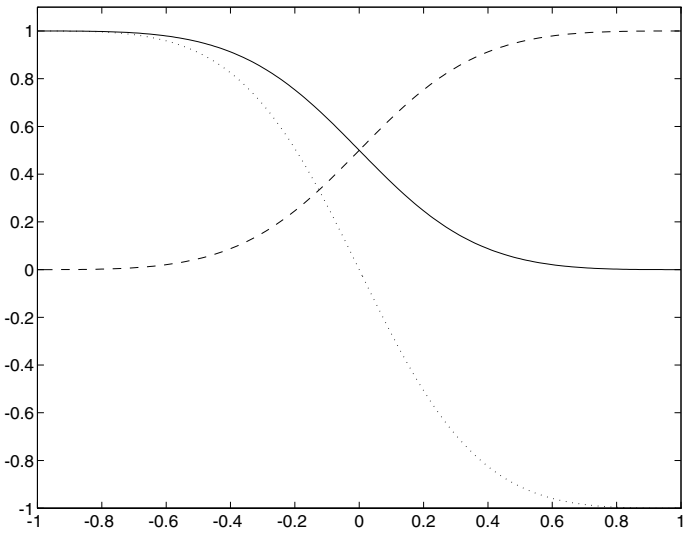

FIGURE 5. Equal parity folding functions: l (full), r (dashed), d (dotted).

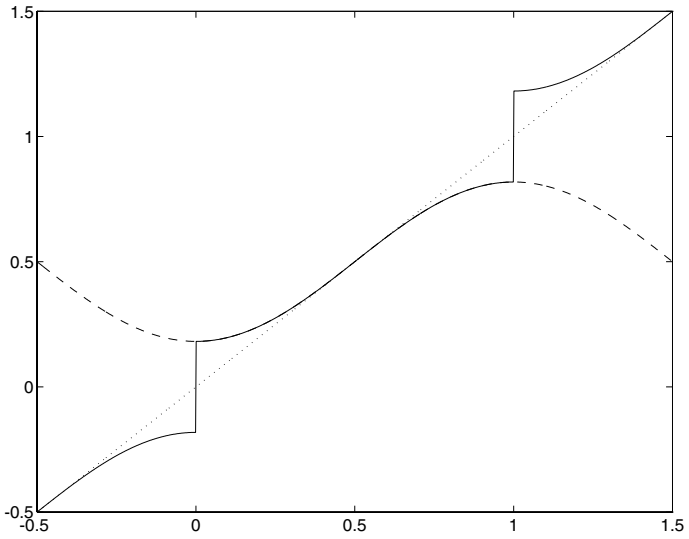

FIGURE 6. Equal parity folding of a linear function.

In the orthogonal construction both discretizations are possible. The fact that a folded function is discontinuous at the folding point does not pose a problem in the nonstaggered discretization. At the folding point we only need the value of the "even" part since we know that the "odd" part vanishes. In the biorthogonal case both options can still be used. In this case the nonstaggered has the disadvantage that the "even–even" intervals contain two more samples than the "odd–odd" intervals. This makes implementation harder.

In the EPF case one has to use the staggered implementation since some of the cut-off functions have a singularity at the folding point. This makes it possible to implement operators that in the

L^2 sense are unbounded or not invertible. The fact that the range of $\mathcal{F}$ is dense in L^2 ensures that these discrete operators are invertible. However, this unavoidably results in ill-conditioned discrete operators. The smaller the grid size, the worse the condition will be.

We next include some numerical examples. Each time we take a function, calculate its transform coefficients, set a certain percentage of the coefficients to zero (the smallest ones), and obtain an approximation by calculating the inverse transform. The errors are measured with the ℓ^2 norm. We always use the staggered discretization.

The first example involves a function that has discontinuities at the folding points. We work on the interval [0, 1] where we assume that the functions are extended periodically to the real line. Consider the function

$$f \;=\; 2 * \chi_{[1/4,3/4)} - 1,$$

which generates a square wave. We take $\frac{1}{4}$ and $\frac{3}{4}$ as folding points, each with $\epsilon = \frac{1}{4}$. We use the staggered discretization with grid size $h = \frac{1}{100}$. After the appropriate local trigonometric transform on each interval, we retain the largest 15% of the coefficients and set the others to zero. We then perform the inverse trigonometric transform and unfolding. Figures 7 and 8 show the folding of f in the biorthogonal and EPF cases and these functions after setting the coefficients to zero (dashed). Figures 9 and 10 then show the unfolding of these functions versus the original function (dashed). As we predicted, the EPF performs poorly in this case.

In a second example we consider a smooth function,

$$f(x) \;=\; e^{-(4x-2)^4},$$

and use the same folding points. Figure 11 gives the norm of the difference between the the original function and the approximation as a function of the percentage of the coefficients that were retained. As we expected, the EPF behaves better here. If the percentage of coefficients kept is less than 15, its error is about 10 times smaller than in the biorthogonal case.

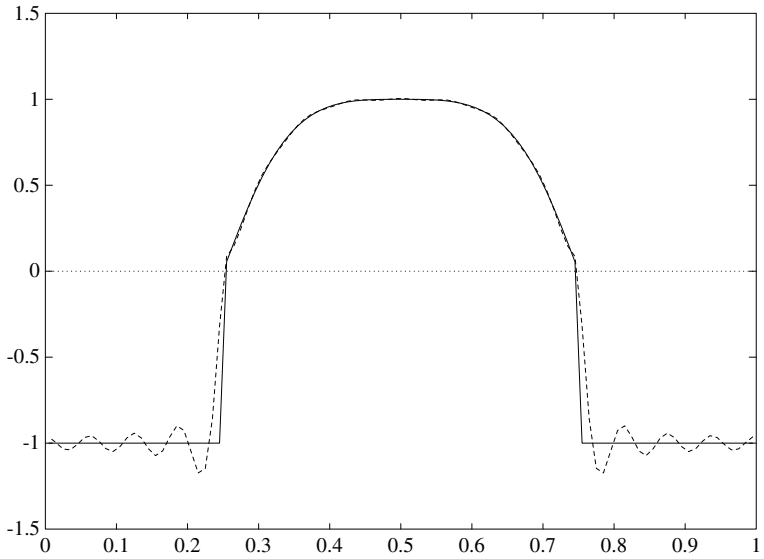

FIGURE 7. Biorthogonal folding of the block and approximation (dashed).

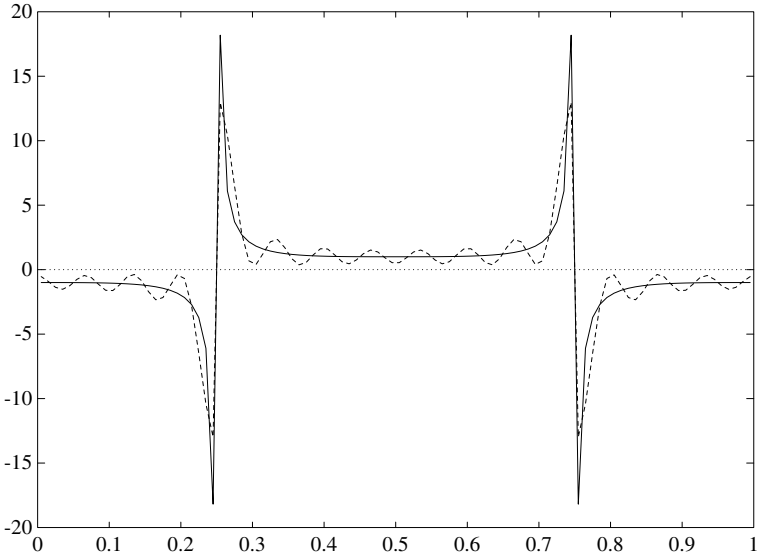

FIGURE 8. Equal parity folding of the block and approximation (dashed).

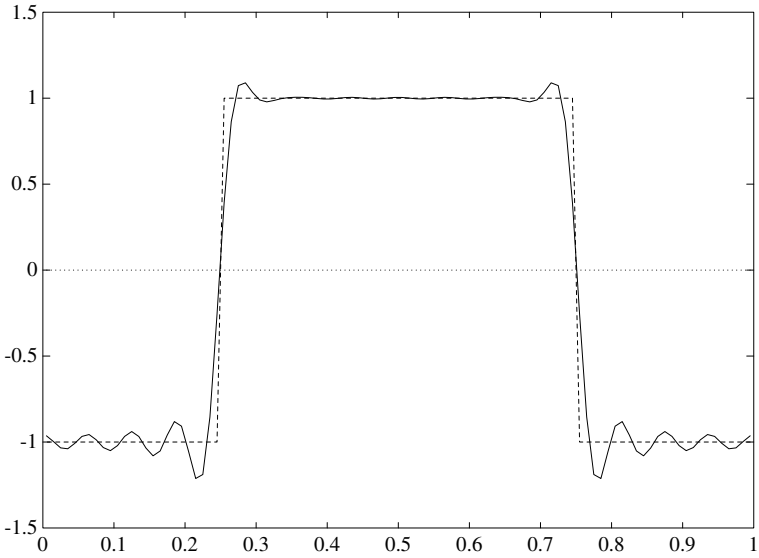

FIGURE 9. Approximation of block wave (biorthogonal case).

10. Image Compression

One of the major applications of smooth local trigonometric bases is image compression. The idea of a transform coding scheme is to take the transform of the image, set the small coefficients to zero, and quantize and encode the other ones. The transform has to be chosen such that it reflects the correlation present in the image. Since images have both spatial and spectral correlation, the basis functions need to be local in space and frequency. A standard still-image compression algorithm is JPEG [19]. The image here is divided into blocks of eight-by-eight pixels, after which the discrete

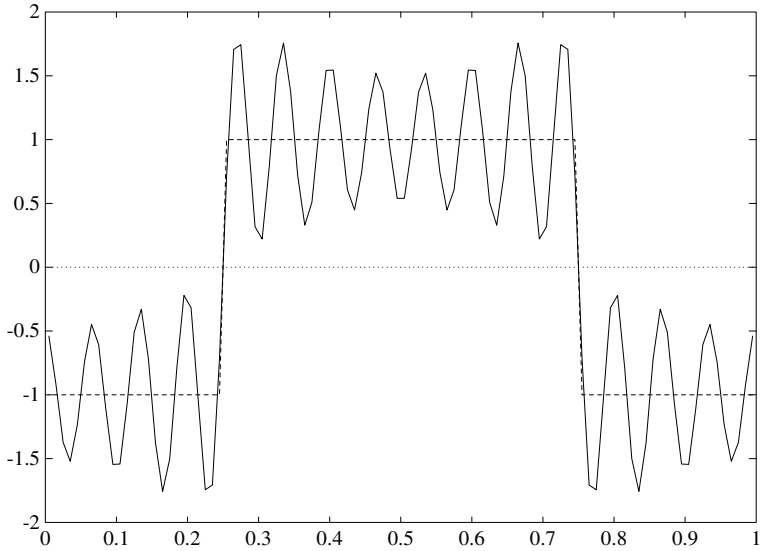

FIGURE 10. Approximation of block wave (EPF case).

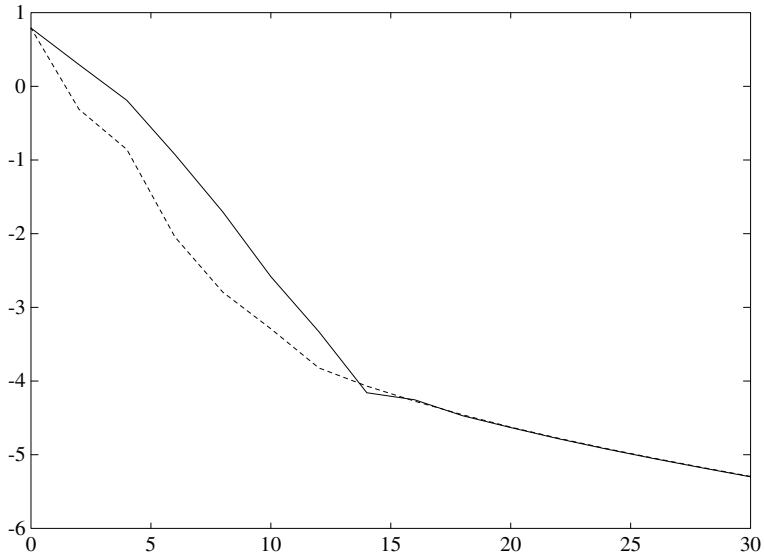

FIGURE 11. Error (logarithmic) as a function of percentage of coefficients. (biorthogonal = full, EPF = dashed).

cosine transform is used on each block. It thus uses a (nonsmooth) local trigonometric basis. One of its disadvantages is that at high compression ratios, the compressed image reveals the splitting location: the so-called blocking effect. This is caused by the fact that the approximations are discontinuous. In [1, 2] *smooth* local trigonometric bases are used for image compression and it is shown that they outperform JPEG. In [11] a comparison between the biorthogonal and the EPF cases is made. The conclusion is that for a fixed compression ratio, EPF has a better SNR but the biorthogonal basis gives better visual image quality.

References

[1] Aharoni, G., Averbuch, A., Coifman, R., and Israeli, M. (1993). Local cosine transform — a method for the reduction of the blocking effect in JPEG. *J. Math. Imag. Vision*, **3**, 7–38.

[2] ———. (1993). Local cosine transform — a method for the reduction of the blocking effect in JPEG. *Mathematical Imaging: Wavelet Applications in Signal and Image Processing*, (A. F. Laine, ed.). Society of Photo-Optical Instrumentation Engineers Proc. Ser., vol. 1034, 205–217.

[3] Auscher, P. (1993). Remarks on the local Fourier bases. *Wavelets: Mathematical Applications* (J. Benedetto and M. Frazier, eds.). CRC Press, Boca Raton, FL, 203–218.

[4] Auscher, P., Weiss, G., and Wickerhauser, V. (1992). Local sine and cosine bases of Coifman and Meyer and the construction of smooth wavelets. *Wavelets: A Tutorial in Theory and Applications* (C. K. Chui, ed.). Academic Press, San Diego, CA, 237–256.

[5] Benedetto, J., and Frazier, M., (eds.). (1993). *Wavelets: Mathematics and Applications*. CRC Press, Boca Raton, FL.

[6] Chui, C. K., (ed.). (1992). *Wavelets: A Tutorial in Theory and Applications*. Academic Press, San Diego, CA.

[7] Coifman, R., and Meyer, Y. (1991). Remarques sur l'analyse de Fourier à fenêtre. *C. R. Acad. Sci. Paris Sér. I Math.*, **312**, 259–261.

[8] Coifman, R. R., and Wickerhauser, M. L. (1992). Entropy based algorithms for best basis selection. *IEEE Trans. Inform. Theory*, **38**, 713–718.

[9] Daubechies, I., Jaffard, S., and Journé, J. L. (1991). A simple Wilson orthonormal basis with exponential decay. *SIAM J. Math. Anal.*, **22**, 554–572.

[10] Fang, X., and Séré, E. (1994). Adaptive multiple folding local trigonometric transforms and wavelet packets. *Appl. Comput. Harmonic. Anal.*, **1**.

[11] Jawerth, B., Liu, Y., and Sweldens, W. (1994). Signal compression with smooth local trigonometric bases. *Opt. Eng.*, **33**, 2125–2135.

[12] Malvar, H. S. (1990). Lapped transforms for efficient transform/subband coding. *IEEE Trans. Acoust. Speech Signal Process.*, **38**, 969–978.

[13] Malvar, H. S., and Staelin, D. H. (1989). The LOT: Transform coding without blocking effects. *IEEE Trans. Acoust. Speech Signal Process.*, **37**, 553–559.

[14] Matviyenko, G. (1994). Optimized local trigonometric bases. Technical Report YALEU/DCS/RR-1041, Department of Computer Science, Yale University.

[15] Meyer, Y. (1990). *Ondelettes et Opérateurs,* I: *Ondelettes,* II: *Opérateurs de Calderón-Zygmund,* III: (with R. Coifman) *Opérateurs multilinéaires*. Hermann, Paris; English transl: I: *Wavelets and Operators*, Cambridge University Press, London, 1993.

[16] Press, W. H., Flannery, B. P., Teukolsky, S. A., and Vetterling, W. T. (1993). *Numerical Recipes*. 2nd ed. Cambridge University Press, London.

[17] Sweldens, W. (1994). *Construction and Applications of Wavelets in Numerical Analysis*. Ph.D. thesis, Department of Computer Science, Katholieke Universiteit Leuven, Belgium.

[18] Walker, J. S. (1991). *Fast Fourier Transforms*. Stud. in Adv. Math. CRC Press, Boca Raton, FL.

[19] Wallace, G. K. (1991). The JPEG still picture compression standard. *Comm. ACM*, **34** 30–44.

[20] Wickerhauser, M. V. (1994). *Adapted Wavelet Analysis from Theory to Software*. A. K. Peters, Wellesley, MA.

[21] Zygmund, A. (1959). *Trigonometric Series*, 2nd ed. Cambridge University Press, London.

Received September 27, 1994

Department of Mathematics, University of South Carolina, Columbia, South Carolina 29208
(jawerth@math.sc.edu)

Department of Mathematics, University of South Carolina, Columbia, South Carolina 29208
and Department of Computer Science, K. U. Leuven, Belgium

Current address: AT&T Bell Laboratories, 600 Mountain Avenue, Rm. 2C-371, Murray Hill, NJ 07974
(wim@research.att.com)